Appears in the Proceedings of IEEE MILCOM'07, October 2007.

3-D Simulation Models for Wideband MIMO Mobile-to-Mobile Channels

Alenka G. Zajić and Gordon L. Stüber
School of Electrical and Computer Engineering
Georgia Institute of Technology, Atlanta, GA 30332 USA

***Abstract*— This article presents a three-dimensional mathematical reference model for wideband multiple-input multiple-output (MIMO) mobile-to-mobile (M-to-M) channels. Based on this model, two sum-of-sinusoids based simulation models are proposed for 3-D wideband MIMO M-to-M multipath-fading channels. The statistics of the simulation models are derived and verified by simulation.**

I. Introduction

Mobile-to-mobile (M-to-M) radio propagation channels arise in inter-vehicular communications, mobile ad-hoc wireless networks, and relay-based cellular radio networks. The statistical properties of M-to-M channels are quite different from conventional fixed-to-mobile (F-to-M) cellular land mobile radio channels [1], [2]. M-to-M communication systems are equipped with low elevation antennas and have both the transmitter ($\mathrm{T_x}$) and receiver ($\mathrm{R_x}$) in motion. Akki and Haber [1], [2] proposed a reference model for single-input single-output (SISO) M-to-M Rayleigh fading channels. The reference models for narrowband multiple-input multiple-output (MIMO) M-to-M channels have been proposed in [3], [4]. Simulation models for MIMO M-to-M channels have been proposed in [5], [6]. All these models assume that the field incident on the $\mathrm{T_x}$ or $\mathrm{R_x}$ antenna is composed of a number of waves travelling only in the *horizontal* plane. This assumption does not seem appropriate for an urban environment where the $\mathrm{T_x}$ and $\mathrm{R_x}$ antenna arrays are often located in close proximity to and lower than surrounding buildings. Recently, we proposed a three-dimensional (3-D) reference model for *narrowband* MIMO M-to-M multipath fading channels [7].

This article presents a 3-D mathematical reference model for *wideband* MIMO M-to-M channels. To describe our 3-D reference model, we first introduce a 3-D geometrical model for wideband MIMO M-to-M channels, referred to as the "concentric-cylinders" model. From the 3-D reference model, the space-time-frequency correlation function for a 3-D non-isotropic scattering environment is derived. The reference models assume an infinite number of scatterers, which prevents practical implementation. Hence, we first propose an ergodic statistical (deterministic) sum-of-sinusoids (SoS) simulation model for a 3-D non-isotropic scattering environment. The statistical properties of our model are verified by simulations. Deterministic simulators are often used because they are easy to implement and have short simulation times. However, they do not reflect the practical channel realizations because their scatterers are placed at specific sights for all simulation trials. By allowing the phases, Doppler frequencies, and time delays to be random variables, the deterministic model is modified to better match statistical properties of the reference model. This model is called the statistical simulation model. The statistical properties of this (statistical) model vary for each simulation trial, but will converge to desired ensemble averaged properties when averaged over a sufficient number of simulation trials. The statistical properties of this model are also verified by simulations. Compared to the deterministic model, the statistical properties of the statistical model match those of the reference model over a wider range of normalized time delays while using smaller number of scatterers.

The remainder of the paper is organized as follows. Section II introduces the "concentric-cylinders" model and presents the 3-D reference model for wideband MIMO M-to-M channels. Section III derives the space-time-frequency correlation function for 3-D non-isotropic scattering. Section IV details the deterministic and statistical SoS simulation models. Section V presents simulation results and, finally, Section VI provides some concluding remarks.

II. A 3-D Reference Model for Wideband MIMO Mobile-to-Mobile Channels

This paper considers a wideband MIMO communication system with L_t transmit and L_r receive omnidirectional antenna elements. It is assumed that both the $\mathrm{T_x}$ and $\mathrm{R_x}$ are in motion and equipped with low elevation antennas. The radio propagation is characterized by 3-D wide sense stationary uncorrelated scattering (WSSUS) with non-line-of-sight (NLoS) conditions between the $\mathrm{T_x}$ and $\mathrm{R_x}$. The MIMO channel can be described by an $L_r \times L_t$ matrix $\mathbf{H}(t,\tau) = [h_{ij}(t,\tau)]_{L_r \times L_t}$ of the input delay-spread functions.

First, we introduce a 3-D geometrical model for wideband MIMO M-to-M channels, called the "concentric-cylinders" model. The "concentric-cylinders" model is an extension of the "two-cylinder" model for narrowband M-to-M channels proposed in [7]. Fig. 1 shows the "concentric-cylinders" model for a wideband MIMO M-to-M channel with $L_t = L_r = 2$ antenna elements. The "concentric-cylinders" model defines

0
Prepared through collaborative participation in the Collaborative Technology Alliance for Communications & Networks sponsored by the U.S. Army Research Laboratory under Cooperative Agreement DAAD19-01-2-0011. The U.S. Government is authorized to reproduce and distribute reprints for Government purposes notwithstanding any copyright notation thereon.

four cylinders, two around the $\mathrm{T_x}$ and another two around the $\mathrm{R_x}$, as shown in Fig. 1. Around the transmitter, M fixed

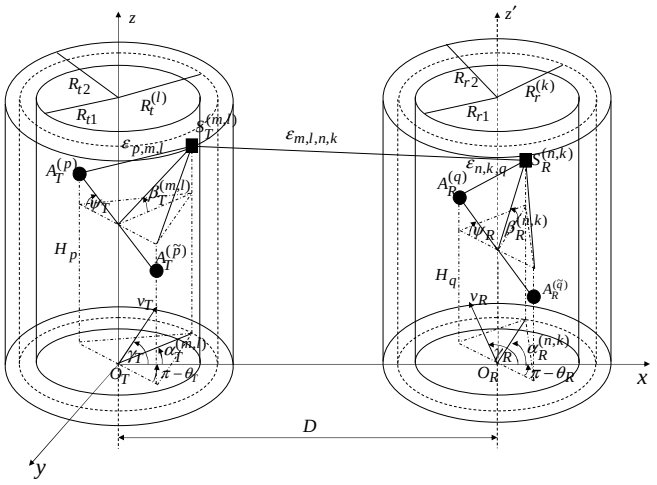

Fig. 1. The "concentric-cylinders" model for wideband MIMO M-to-M channel with $L_t = L_r = 2$ antenna elements.

omnidirectional scatterers occupy a volume between cylinders of radii R_{t1} and R_{t2}. It is assumed that the M scatterers lie on L cylindric surfaces of radii $R_{t1} \leq R_t^{(l)} \leq R_{t2}$, where $1 \leq l \leq L$. The l^{th} cylindric surface contains $M^{(l)}$ fixed omnidirectional scatterers, and the $(m,l)^{th}$ transmit scatterer is denoted by $S_T^{(m,l)}$. Similarly, around the receiver, N fixed omnidirectional scatterers occupy a volume between cylinders of radii R_{r1} and R_{r2}. It is assumed that N scatterers lie on K cylindric surfaces of radii $R_{r1} \leq R_r^{(k)} \leq R_{r2}$, where $1 \leq k \leq K$. The k^{th} cylindric surface contains $N^{(k)}$ fixed omnidirectional scatterers, and the $(n,k)^{th}$ receive scatterer is denoted by $S_R^{(n,k)}$. The distance between the centers of the $\mathrm{T_x}$ and $\mathrm{R_x}$ cylinders is D. It is assumed that $\max\{R_{t2}, R_{r2}\} \ll D$ (local scattering condition) and $D <= 4R_{t1}R_{r1}L_r/(\lambda(L_t - 1)(L_r - 1))$ (channel does not experience keyhole behavior [8]), where λ denotes the carrier wavelength. The spacing between antenna elements at the $\mathrm{T_x}$ and $\mathrm{R_x}$ is denoted by d_T and d_R, respectively. It is assumed that d_T and d_R are much smaller than the radii R_{t1} and R_{r1}, i.e., $\max\{d_T, d_R\} \ll \min\{R_{t1}, R_{r1}\}$. Angles θ_T and θ_R describe the orientation of the $\mathrm{T_x}$ and $\mathrm{R_x}$ antenna array in the x - y plane, respectively, relative to the x - axis. Similarly, angles ψ_T and ψ_R describe the elevation of the $\mathrm{T_x}$'s antenna array and the $\mathrm{R_x}$'s antenna array relative to the x - y plane, respectively. The $\mathrm{T_x}$ and $\mathrm{R_x}$ are moving with speeds v_T and v_R in directions described by angles γ_T and γ_R, respectively. The symbols $\alpha_T^{(m,l)}$ and $\alpha_R^{(n,k)}$ denote the azimuth angle of departure (AAoD) and the azimuth angle of arrival (AAoA), respectively. Similarly, the symbols $\beta_T^{(m,l)}$ and $\beta_R^{(n,k)}$ denote the elevation angle of departure (EAoD) and the elevation angle of arrival (EAoA), respectively. Finally, the symbols $\epsilon_{p,m,l}$, $\epsilon_{m,l,n,k}$, and $\epsilon_{n,k,q}$ denote distances $A_T^{(p)}$ - $S_T^{(m,l)}$, $S_T^{(m,l)}$ - $S_R^{(n,k)}$, and $S_R^{(n,k)}$ - $A_R^{(q)}$, respectively, as shown in Fig. 1.

In the 3-D reference model, the number of local scatterers around the $\mathrm{T_x}$ and $\mathrm{R_x}$ is infinite. Consequently, the input delay-spread function of the link $A_T^{(p)} - A_R^{(q)}$ is

$$h_{pq}(t,\tau) = \lim_{M,N\to\infty} \sum_{l,m=1}^{L,M^{(l)}} \sum_{k,n=1}^{K,N^{(k)}} \eta_{l,k}\, g_{m,l,n,k}(t)\, \delta(\tau - \tau_{m,l,n,k}), \quad (1)$$

where parameters $\eta_{l,k}$, $\tau_{m,l,n,k}$ denote amplitudes of the multipath components and time delays, respectively. Function $g_{m,l,n,k}(t)$ is defined as follows

$$g_{m,l,n,k}(t) = e^{-j\frac{2\pi}{\lambda}(\epsilon_{p,m,l}+\epsilon_{m,l,n,k}+\epsilon_{n,k,q})+j\phi_{m,l,n,k}} \times e^{j2\pi t[f_{T\max}\cos(\alpha_T^{(m,l)}-\gamma_T)+f_{R\max}\cos(\alpha_R^{(n,k)}-\gamma_R)]}, \quad (2)$$

where $f_{T\max} = v_T/\lambda$ and $f_{R\max} = v_R/\lambda$ are the maximum Doppler frequencies associated with the $\mathrm{T_x}$ and $\mathrm{R_x}$, respectively, and λ is the carrier wavelength. The amplitude of the multipath component, $\eta_{l,k}$, is defined as

$$\begin{aligned} \eta_{l,k} &= \frac{\sqrt{P_{pq}}\lambda}{4\pi\sqrt{M^{(l)}N^{(k)}}}\left(R_t^{(l)} + D + R_r^{(k)}\right)^{-\gamma/2} \\ &\approx \Omega_{pq}\left(1 - \frac{\gamma}{2}\frac{R_t^{(l)} + R_r^{(k)}}{2D}\right), \end{aligned} \quad (3)$$

where P_{pq} denotes the power transmitted through the sub-channel $A_T^{(p)} - A_R^{(q)}$, γ is the path loss exponent, and $\Omega_{pq} = D^{-\gamma/2}\sqrt{P_{pq}}\lambda/\left(4\pi\sqrt{M^{(l)}N^{(k)}}\right)$. Finally, the time delay $\tau_{m,l,n,k}$ is defined as the travel time of the wave impinged on the scatterer $S_T^{(m,l)}$ and scattered from the scatterer $S_R^{(n,k)}$, i.e., $\tau_{m,l,n,k} = D/c_0 + R_t^{(l)}(1 - \cos\alpha_T^{(m,l)})/c_0\cos\beta_T^{(m,l)} + R_r^{(k)}(1 + \cos\alpha_R^{(n,k)})/c_0\cos\beta_R^{(n,k)}$, where c_0 is the speed of light. It is assumed that the angles of departures (AAoDs and EAoDs), the angles of arrivals (AAoAs and EAoAs), and the radii $R_t^{(l)}$ and $R_r^{(k)}$ are random variables. Since all rays are double-bounced, the angles of departure and radii $R_t^{(l)}$ are independent from the angles of arrival and radii $R_r^{(k)}$ [8]. Additionally, it is assumed that the phases ϕ_{mn} are random variables uniformly distributed on the interval $[-\pi, \pi)$ and independent from the angles of departure, the angles of arrival, and the radii of the cylinders.

The distances $\epsilon_{p,m,l}$, $\epsilon_{n,k,q}$, and $\epsilon_{m,l,n,k}$ can be expressed as functions of the random variables $\alpha_T^{(m,l)}$, $\alpha_R^{(n,k)}$, $\beta_T^{(m,l)}$, $\beta_R^{(n,k)}$, $R_t^{(l)}$, and $R_r^{(k)}$ as follows:

$$\begin{aligned} \epsilon_{p,m,l} &\approx R_t^{(l)}/\cos\beta_T^{(m,l)} - (0.5L_t + 0.5 - p)\big[d_{Tz}\sin\beta_T^{(m,l)} \\ &+ d_{Tx}\cos\alpha_T^{(m,l)}\cos\beta_T^{(m,l)} + d_{Ty}\sin\alpha_T^{(m,l)}\cos\beta_T^{(m,l)}\big], \end{aligned} \quad (4)$$

$$\begin{aligned} \epsilon_{n,k,q} &\approx R_r^{(k)}/\cos\beta_R^{(n,k)} - (0.5L_r + 0.5 - q)\big[d_{Rz}\sin\beta_R^{(n,k)} \\ &+ d_{Rx}\cos\alpha_R^{(n,k)}\cos\beta_R^{(n,k)} + d_{Ry}\sin\alpha_R^{(n,k)}\cos\beta_R^{(n,k)}\big], \end{aligned} \quad (5)$$

$$\epsilon_{m,l,n,k} \approx D, \quad (6)$$

where parameters p and q take values from the sets $p \in \{1,\ldots,L_t\}$ and $q \in \{1,\ldots,L_r\}$, $d_{Tx} = d_T\cos\psi_T\cos\theta_T$, $d_{Ty} = d_T\cos\psi_T\sin\theta_T$, $d_{Rx} = d_R\cos\psi_R\cos\theta_R$, $d_{Ry} = d_R\cos\psi_R\sin\theta_R$, $d_{Tz} = d_T\sin\psi_T$, and $d_{Rz} = d_R\sin\psi_R$. Derivations of expressions (4) - (6) are omitted for brevity.

In further derivations we will use the time-variant transfer function instead of the input delay-spread function. The time-variant transfer function is defined as the Fourier transformation of the input delay-spread function and using (1) - (6) can be written as

$$T_{pq}(t,f) = \mathcal{F}_\tau\left\{h_{pq}(t,\tau)\right\} = \lim_{M,N\to\infty} \sum_{l,m,k,n=1}^{L,M^{(l)},K,N^{(k)}} e^{j\phi_{m,l,n,k} - j\frac{2\pi}{c_0} fD} \quad (7)$$

$$\Omega_{pq}\left(1 - \frac{\gamma}{2}\frac{R_t^{(l)} + R_r^{(k)}}{2D}\right) a_{p,m,l} b_{n,k,q} e^{j2\pi t f_{T\max}\cos(\alpha_T^{(m,l)} - \gamma_T)}$$

$$e^{j2\pi t f_{R\max}\cos(\alpha_R^{(n,k)} - \gamma_R) - j\frac{2\pi}{c_0} f\left[\frac{R_t^{(l)}(1-\cos\alpha_T^{(m,l)})}{\cos\beta_T^{(m,l)}} + \frac{R_r^{(k)}(1+\cos\alpha_R^{(n,k)})}{\cos\beta_R^{(n,k)}}\right]},$$

where parameters $a_{p,m,l}$ and $b_{n,k,q}$ are defined as

$$\begin{aligned} a_{p,m,l} &= e^{-j\frac{2\pi}{\lambda}(D/2+R_t^{(l)}) + j\frac{\pi}{\lambda}(L_t+1-2p)d_{Tz}\sin\beta_T^{(m,l)}} \quad (8)\\ &\times\ e^{j\frac{\pi}{\lambda}(L_t+1-2p)\cos\beta_T^{(m,l)}(d_{Tx}\cos\alpha_T^{(m,l)} + d_{Ty}\sin\alpha_T^{(m,l)})}, \\ b_{n,k,q} &= e^{-j\frac{2\pi}{\lambda}(D/2+R_r^{(k)}) + j\frac{\pi}{\lambda}(L_r+1-2q)d_{Rz}\sin\beta_R^{(n,k)}} \quad (9)\\ &\times\ e^{j\frac{\pi}{\lambda}(L_r+1-2q)\cos\beta_R^{(n,k)}(d_{Rx}\cos\alpha_R^{(n,k)} + d_{Ry}\sin\alpha_R^{(n,k)})}. \end{aligned}$$

III. Space-Time-Frequency Correlation Function of the 3-D Reference Model

Assuming a 3-D non-isotropic scattering environment, we now derive the space-time-frequency correlation function of the 3-D reference model. The normalized space-time-frequency correlation function between two time-variant transfer functions $T_{pq}(t,f)$ and $T_{\tilde{p}\tilde{q}}(t,f)$ is defined as

$$R_{pq,\tilde{p}\tilde{q}}[\Delta t, \Delta f] = \frac{\mathrm{E}\left[T_{pq}^*(t,f)T_{\tilde{p}\tilde{q}}(t+\Delta t, f+\Delta f)\right]}{\sqrt{\mathrm{E}[|T_{pq}(t,f)|^2]\mathrm{E}[|T_{\tilde{p}\tilde{q}}(t,f)|^2]}}, \quad (10)$$

where $(\ \cdot\ )^*$ denotes complex conjugate operation, $\mathrm{E}[\ \cdot\ ]$ is the statistical expectation operator, $p,\tilde{p} \in \{1,\ldots,L_t\}$, and $q,\tilde{q} \in \{1,\ldots,L_r\}$. Since the number of local scatterers in the reference model described in Section II is infinite, the discrete AAoDs, $\alpha_T^{(m,l)}$, EAoDs, $\beta_T^{(m,l)}$, AAoAs, $\alpha_R^{(n,k)}$, EAoAs, $\beta_R^{(n,k)}$, and radii $R_t^{(l)}$ and $R_r^{(k)}$ can be replaced with continuous random variables α_T, β_T, α_R, β_R, R_t, and R_r with probability density functions (pdfs) $f(\alpha_T)$, $f(\beta_T)$, $f(R_t)$, $f(\alpha_R)$, $f(\beta_R)$, and $f(R_r)$, respectively. Several different scatterer distributions, such as uniform, Gaussian, Laplacian, and von Mises, are used in prior work to characterize the random azimuth angles α_T and α_R. In this paper, we use the von Mises pdf because it approximates many of the previously mentioned distributions and leads to closed-form solutions for many useful situations. The von Mises pdf is defined in [9] as $f(\theta) = \exp\left[k\cos(\theta-\mu)\right]/(2\pi I_0(k))$, where $\theta \in [-\pi,\pi)$, $I_0(\ \cdot\ )$ is the zeroth-order modified Bessel function of the first kind, $\mu \in [-\pi,\pi)$ is the mean angle at which the scatterers are distributed in the x - y plane, and k controls the spread of scatterers around the mean. Prior work uses several different scatterer distributions, such as uniform, cosine, and Gaussian, to characterize the random elevation angles β_T and β_R. Here, we use the pdf [10]

$$f(\varphi) = \begin{cases} \frac{\pi}{4\varphi_m}\cos\left(\frac{\pi}{2}\frac{\varphi}{\varphi_m}\right) & ,\ |\ \varphi\ | \le \varphi_m \le \frac{\pi}{2} \\ 0 & ,\ \text{otherwise} \end{cases}, \quad (11)$$

because it matches well the experimental data in [11]. Parameter φ_m is the absolute value of the maximum elevation angle and lies in the range $0^\circ \le \varphi_m \le 20^\circ$ [11]. To characterize the radii R_t and R_r we use the pdfs $f(R_t) = 2R_t/(R_{t2}^2 - R_{t1}^2)$ and $f(R_r) = 2R_r/(R_{r2}^2 - R_{r1}^2)$, respectively. This pdf is selected because it matches well the experimental data in [12]. Using trigonometric transformations, the equality $\int_{-\pi}^{\pi}\exp\left\{a\sin(c) + b\cos(c)\right\}dc = 2\pi I_0\left(\sqrt{a^2+b^2}\right)$ [13, eq. 3.338-4], and the results in [7], the space-time-frequency correlation function can be closely approximated as

$$\begin{aligned} R_{pq,\tilde{p}\tilde{q}}[d_T, d_R, \Delta t, \Delta f] \approx\ & A_T \int_{R_{t1}}^{R_{t2}} e^{-j\frac{2\pi}{c_0}\Delta f R_t} I_0\left(\sqrt{x^2+y^2}\right) 2R_t dR_t \\ \times\ & A_R \int_{R_{r1}}^{R_{r2}} \left(1 - \gamma\frac{R_r}{D}\right) e^{-j\frac{2\pi}{c_0}\Delta f R_r} I_0\left(\sqrt{w^2+z^2}\right) R_r dR_r \\ +\ & A_T \int_{R_{t1}}^{R_{t2}} \left(1 - \gamma\frac{R_t}{D}\right) e^{-j\frac{2\pi}{c_0}\Delta f R_t} I_0\left(\sqrt{x^2+y^2}\right) R_t dR_t \\ \times\ & A_R \int_{R_{r1}}^{R_{r2}} e^{-j\frac{2\pi}{c_0}\Delta f R_r} I_0\left(\sqrt{w^2+z^2}\right) 2R_r dR_r, \end{aligned} \quad (12)$$

where parameters A_T, A_R, x, y, z, and w are

$$\begin{aligned} A_T &= \frac{e^{-j\pi\Delta f D/c_0}}{I_0(k_T)} \frac{\cos(\frac{2\pi}{\lambda}\beta_{T_m}(p-\tilde{p})d_{T_z})}{1 - \left(\frac{4\beta_{T_m}(p-\tilde{p})d_{T_z}}{\lambda}\right)^2} \frac{1}{R_{t2}^2 - R_{t1}^2}, \\ A_R &= \frac{e^{-j\pi\Delta f D/c_0}}{I_0(k_R)} \frac{\cos(\frac{2\pi}{\lambda}\beta_{R_m}(q-\tilde{q})d_{R_z})}{1 - \left(\frac{4\beta_{R_m}(q-\tilde{q})d_{R_z}}{\lambda}\right)^2} \frac{1}{R_{r2}^2 - R_{r1}^2}, \end{aligned}$$

$x = j2\pi(p-\tilde{p})d_{T_x}/\lambda + j2\pi\Delta t f_{T\max}\cos\gamma_T + j2\pi\Delta f R_t/c_0 + k_T\cos\mu_T$, $y = j2\pi(p-\tilde{p})d_{T_y}/\lambda + j2\pi\Delta t f_{T\max}\sin\gamma_T + k_T\sin\mu_T$, $z = j2\pi(q-\tilde{q})d_{R_x}/\lambda + j2\pi\Delta t f_{R\max}\cos\gamma_R - j2\pi\Delta f R_r/c_0 + k_R\cos\mu_R$, $w = j2\pi(q-\tilde{q})d_{R_y}/\lambda + j2\pi\Delta t f_{R\max}\sin\gamma_R + k_R\sin\mu_R$. To obtain the space-time-frequency correlation function for the 3-D MIMO M-to-M system, the integrals in (12) must be evaluated numerically, because they do not have closed-form solutions.

IV. Wideband MIMO Mobile-to-Mobile Simulation Models

The reference model for wideband MIMO M-to-M channel described in Section II assumes an infinite number of scatterers, which prevents practical implementation. It is desirable to design simulation models with a finite number of scatterers, while still matching the statistical properties of the reference model. Assuming 3-D non-isotropic scattering, using the reference model described in Section II, and using the results in [14], we propose the following function as a time-variant transfer function: $T_{pq}(t,f) = T_{pq}^{(I)}(t,f) + jT_{pq}^{(Q)}(t,f)$ where

$$T_{pq}^{(I)}(t,f) = \sum_{l,m,i,k,n,g=1}^{L,M_A^{(l)},M_E^{(l)},K,N_A^{(k)},N_E^{(k)}} \frac{1}{\sqrt{M_A^{(l)}M_E^{(l)}N_A^{(k)}N_E^{(k)}}} \quad (13)$$

$$\times \left(1-\frac{\gamma}{2}\frac{R_t^{(l)}+R_r^{(k)}}{2D}\right)\cos\Bigg\{K_pD_T+K_qD_R+2\pi t f_{T\max}$$
$$\times\cos\left(\alpha_T^{(m,l)}-\gamma_T\right)+2\pi t f_{R\max}\cos\left(\alpha_R^{(n,k)}-\gamma_R\right)+\phi_{m,i,l,n,g,k}$$
$$-\frac{2\pi}{c_0}f\Bigg[D+R_t^{(l)}\left(1-\cos\alpha_T^{(m,l)}\right)+R_r^{(k)}\left(1+\cos\alpha_R^{(n,k)}\right)\Bigg]\Bigg\},$$

$$T_{pq}^{(Q)}(t,f)=\sum_{l,m,i,k,n,g=1}^{L,M_A^{(l)},M_E^{(l)},K,N_A^{(k)},N_E^{(k)}}\frac{1}{\sqrt{M_A^{(l)}M_E^{(l)}N_A^{(k)}N_E^{(k)}}} \quad (14)$$
$$\times \left(1-\frac{\gamma}{2}\frac{R_t^{(l)}+R_r^{(k)}}{2D}\right)\sin\Bigg\{K_pD_T+K_qD_R+2\pi t f_{T\max}$$
$$\times\cos\left(\alpha_T^{(m,l)}-\gamma_T\right)+2\pi t f_{R\max}\cos\left(\alpha_R^{(n,k)}-\gamma_R\right)+\phi_{m,i,l,n,g,k}$$
$$-\frac{2\pi}{c_0}f\Bigg[D+R_t^{(l)}\left(1-\cos\alpha_T^{(m,l)}\right)+R_r^{(k)}\left(1+\cos\alpha_R^{(n,k)}\right)\Bigg]\Bigg\},$$

are the in-phase (I) and quadrature (Q) components of the time-variant transfer function, $M^{(l)}=M_A^{(l)}M_E^{(l)}$, $N^{(k)}=N_A^{(k)}N_E^{(k)}$, $K_p=\pi(L_t+1-2p)/\lambda$, $K_q=\pi(L_r+1-2q)/\lambda$,$D_T=d_{Tx}\cos\alpha_T^{(m,l)}+d_{Ty}\sin\alpha_T^{(m,l)}+d_{Tz}\sin\beta_T^{(i,l)}$, and $D_R=d_{Rx}\cos\alpha_R^{(n,k)}+d_{Ry}\sin\alpha_R^{(n,k)}+d_{Rz}\sin\beta_R^{(g,k)}$. Note that the input delay-spread function can be obtained as the inverse Fourier transformation of the time-variant transfer function, i.e. $h_{pq}(t,\tau)=\mathcal{F}_f^{-1}\{T_{pq}(t,f)\}$.

A. Deterministic Wideband MIMO M-to-M Simulation Model

First, we propose an ergodic statistical (deterministic) model. This model has only phases as random variables and needs only one simulation trial to obtain the desired statistical properties. The time-variant transfer function is $T_{pq}(t,f)=T_{pq}^{(I)}(t,f)+jT_{pq}^{(Q)}(t,f)$, where functions $T_{pq}^{(I)}(t,f)$ and $T_{pq}^{(Q)}(t,f)$ are defined in (13) and (14). The AAoDs, $\alpha_T^{(m,l)}$, and the AAoAs, $\alpha_R^{(n,k)}$, are modelled using the von Mises pdf and are generated as follows:

$$\alpha_T^{(m,l)}=F^{-1}\left(\frac{m-0.5}{M_A^{(l)}}\right),\alpha_R^{(n,k)}=F^{-1}\left(\frac{n-0.5}{N_A^{(k)}}\right), \quad (15)$$

for $m=1,\ldots,M_A^{(l)}$, $n=1,\ldots,N_A^{(k)}$, where $F(\ \cdot\ )^{-1}$ denotes the inverse cumulative von Mises distribution function and is evaluated using method in [15]. The EAoDs, $\beta_T^{(m,l)}$, and the EAoAs, $\beta_R^{(n,k)}$, are modelled using the pdf in (11) and are generated as follows:

$$\beta_T^{(i,l)} = \frac{2\beta_{T_m}}{\pi}\arcsin\left(\frac{2i-1}{M_E^{(l)}}-1\right), \quad (16)$$

$$\beta_R^{(g,k)} = \frac{2\beta_{R_m}}{\pi}\arcsin\left(\frac{2g-1}{N_E^{(k)}}-1\right), \quad (17)$$

for $i=1,\ldots,M_E^{(l)}$, $g=1,\ldots,N_E^{(k)}$. The radii $R_t^{(l)}$ and $R_r^{(k)}$ are modelled using pdfs $f(R_t)=2R_t/(R_{t2}^2-R_{t1}^2)$ and $f(R_r)=2R_r/(R_{r2}^2-R_{r1}^2)$, respectively, and are generated as follows:

$$R_t^{(l)} = \sqrt{\frac{(l-0.5)(R_{t2}^2-R_{t1}^2)}{L}+R_{t1}^2}, \quad (18)$$

$$R_r^{(k)} = \sqrt{\frac{(k-0.5)(R_{r2}^2-R_{r1}^2)}{K}+R_{r1}^2}, \quad (19)$$

for $l=1,\ldots,L$, $k=1,\ldots,K$. The phases $\phi_{m,i,l,n,g,k}$ are generated as independent random variables uniformly distributed on the interval $[-\pi,\pi)$. For $M,N\to\infty$, our deterministic model can be shown to exhibit property (12) of the reference model. Derivation is omitted for brevity.

B. Statistical Wideband MIMO M-to-M Simulation Model

Deterministic simulators are often used because they are easy to implement and have short simulation times. However, they do not reflect the practical channel realizations because their scatterers are placed at specific sights for all simulation trials. By allowing phases, Doppler frequencies, and time delays to be random variables, our deterministic model can be modified to match statistical properties of the reference model over a wider range of normalized time delays, while at the same time requiring a smaller number of scatterers. The statistical properties of this (statistical) model vary for each simulation trial, but will converge to desired ensemble averaged properties when averaged over a sufficient number of simulation trials.

The time-variant transfer function is $T_{pq}(t,f)=T_{pq}^{(I)}(t,f)+jT_{pq}^{(Q)}(t,f)$, where functions $T_{pq}^{(I)}(t,f)$ and $T_{pq}^{(Q)}(t,f)$ are defined in (13) and (14). The AAoDs, the AAoAs, the EAoDs, the EAoAs, and the radii are generated as follows:

$$\alpha_T^{(m,l)} = F^{-1}\left(\frac{m+\theta_A^{(l)}-1}{M_A^{(l)}}\right), \quad (20)$$

$$\alpha_R^{(n,k)} = F^{-1}\left(\frac{n+\psi_A^{(k)}-1}{N_A^{(k)}}\right), \quad (21)$$

$$\beta_T^{(i,l)} = \frac{2\beta_{T_m}}{\pi}\arcsin\left(\frac{2(i+\theta_E^{(l)}-1)}{M_E^{(l)}}-1\right), \quad (22)$$

$$\beta_R^{(g,k)} = \frac{2\beta_{R_m}}{\pi}\arcsin\left(\frac{2(g+\psi_E^{(k)}-1)}{N_E^{(k)}}-1\right), \quad (23)$$

$$R_t^{(l)} = \sqrt{\frac{(l+\sigma_T-1)(R_{t2}^2-R_{t1}^2)}{L}+R_{t1}^2}, \quad (24)$$

$$R_r^{(k)} = \sqrt{\frac{(k+\sigma_R-1)(R_{r2}^2-R_{r1}^2)}{K}+R_{r1}^2}, \quad (25)$$

for $m=1,\ldots,M_A^{(l)}$, $n=1,\ldots,N_A^{(k)}$, $i=1,\ldots,M_E^{(l)}$, $g=1,\ldots,N_E^{(k)}$, $l=1,\ldots,L$, and $k=1,\ldots,K$ respectively. The parameters $\theta_A^{(l)}$, $\psi_A^{(k)}$, $\theta_E^{(l)}$, $\psi_E^{(k)}$, σ_T, and σ_R are independent random variables uniformly distributed on the interval $[0,1)$. Our statistical model can be shown to exhibit property (12) of the reference model. Derivation is omitted for brevity.

V. Simulation Results

In this section, we present some simulation results to verify theoretical derivations and to compare the simulation models with the reference model proposed in Section II. In all simulations, we use a normalized sampling period $f_{T\max}T_s=0.01$ ($f_{T\max}=f_{R\max}$ are the maximum Doppler frequencies and

T_s is the sampling period). The parameters used to obtain curves in Figs. 2 and 3 are $L_t = L_r = 2$, $\beta_{Tm} = \beta_{Rm} = 15°$, $\theta_T = \theta_R = \pi/4$, $\psi_T = \psi_R = \pi/3$, $\gamma_T = \gamma_R = 20°$, $k_T = k_R = 0$, $\lambda = 0.3$ m, $R_{t1} = R_{r1} = 30$ m, $R_{t2} = R_{r2} = 300$ m, $D = 5000$ m, and $\gamma = 4$.

Fig. 2 compares the Doppler spectra obtained using our reference model (for $d_T = d_R = 0$) with measured Doppler spectra for SISO system. The measured results are taken from Fig. 4(d) of [16]. The close agreement between the theoretical and empirical curves confirms the utility of the proposed wideband model. Fig. 3 compares the space-time-frequency

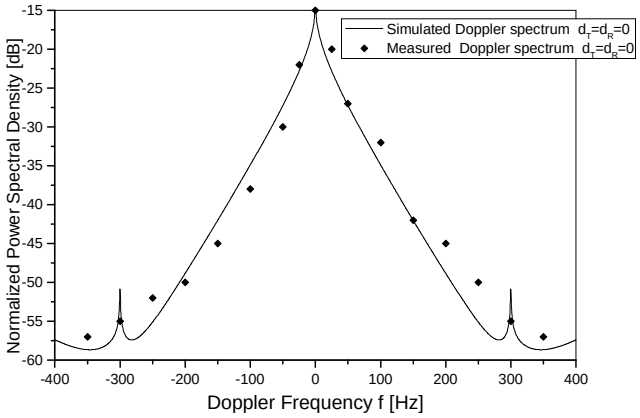

Fig. 2. The normalized simulated and measured Doppler power spectra for SISO system.

correlation functions ($d_T = d_R = 0.5\ \lambda$, $\Delta f = 100$ Hz) of the reference, deterministic, and statistical models. The space-time-frequency correlation function of the deterministic model is obtained with $M_A^{(l)} = 32$, $M_E^{(l)} = 7$, $N_A^{(k)} = 32$, and $N_E^{(k)} = 7$ scatterers and six tap-delays ($L = 3$ and $K = 3$), whereas the space-time-frequency correlation function of the statistical model is obtained with $M_A^{(l)} = 12$, $M_E^{(l)} = 3$, $N_A^{(k)} = 12$, and $N_E^{(k)} = 3$ scatterers, six tap-delays ($L = 3$ and $K = 3$), and $N_{\text{stat}} = 10$ simulation trials. Results show that the space-time-frequency correlation function of the deterministic model closely matches the theoretical one in the range of normalized time delays, $0 \leq f_{T\max} T_s \leq 4$, whereas the space-time correlation function of the statistical model approaches the theoretical one in a wider range of normalized time delays, i.e., $0 \leq f_{T\max} T_s \leq 10$.

VI. Conclusions

In this paper, the 3-D reference model for wideband MIMO M-to-M fading channels is developed. From the reference model, the space-time-frequency correlation function for a 3-D non-isotropic scattering environment is derived. Finally, the deterministic and statistical SoS simulators are presented and shown to closely match the statistical properties of the reference model.

Disclaimer

The views and conclusions contained in this document are those of the authors and should not be interpreted as representing the official policies, either expressed or implied, of the Army Research Laboratory or the U. S. Government.

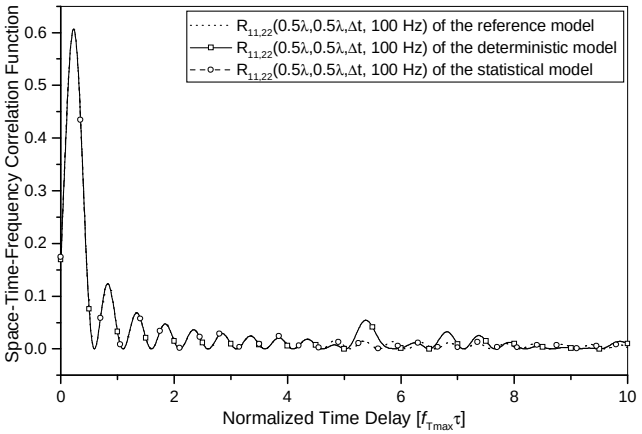

Fig. 3. The normalized space-time-frequency correlation functions ($d_T = d_R = 0.5\ \lambda$, $\Delta f = 100$ Hz) of the reference, deterministic, and statistical models.

References

[1] A.S. Akki and F. Haber, "A statistical model for mobile-to-mobile land communication channel," *IEEE Trans. on Veh. Tech.*, vol. 35, pp. 2–10, Feb. 1986.

[2] A.S. Akki, "Statistical properties of mobile-to-mobile land communication channels," *IEEE Trans. on Veh. Tech.*, vol. 43, pp. 826–831, Nov. 1994.

[3] M. Pätzold, B.O. Hogstad, N. Youssef, and D. Kim, "A MIMO mobile-to-mobile channel model: Part I-the reference model," *Proc. IEEE PIMRC'05*, vol. 1, pp. 573–578, Berlin, Germany, Sept. 2005.

[4] A.G. Zajić and G.L. Stüber, "Space-time correlated MIMO mobile-to-mobile channels," *Proc. IEEE PIMRC'06*, Helsinki, Finland, Sept. 2006.

[5] B.O. Hogstad, M. Pätzold, N. Youssef, and D. Kim, "A MIMO mobile-to-mobile channel model: Part II-the simulation model," *Proc. IEEE PIMRC'05*, vol. 1, pp. 562–567, Berlin, Germany, Sept. 2005.

[6] A.G. Zajić and G.L. Stüber, "Simulation models for MIMO mobile-to-mobile channels," *Proc. IEEE MILCOM*, Washington, D.C., Oct. 2006.

[7] A.G. Zajić and G.L. Stüber, "A three-dimensional MIMO mobile-to-mobile channel model," *IEEE WCNC'07*, Hong Kong, March 2007.

[8] D. Gesbert, H. Bölcskei, D.A. Gore, and A.J. Paulraj, "Outdoor MIMO wireless channels: models and performance prediction," *IEEE Trans. on Commun.*, vol. 50, pp. 1926–1934, Dec. 2002.

[9] A. Abdi, J. A. Barger, and M. Kaveh, "A parametric model for the distribution of the angle of arrival and the associated correlation function and power spectrum at the mobile station," *IEEE Trans. on Veh. Tech.*, vol. 51, pp. 425–434, May 2002.

[10] J.D. Parsons and A.M.D. Turkmani, "Characterisation of mobile radio signals: model description," *IEE Proc. I, Commun., Speach, and Vision*, vol. 138, pp. 549–556, Dec. 1991.

[11] Y. Yamada, Y. Ebine, and N. Nakajima, "Base station/vehicular antenna design techniques employed in high capacity land mobile communications system," *Rev. Elec. Commun. Lab.*, NTT, pp. 115–121, 1987.

[12] K.I. Pedersen, P.E. Mogensen, and B.H. Fleury, "A stochastic model of the temporal and azimuthal dispersion seen at the base station in outdoor propagation environments," *IEEE Trans. on Veh. Tech.*, vol. 49, pp. 437–447, March 2000.

[13] I.S. Gradshteyn and I.M. Ryzhik, *Table of Integrals, Series, and Products* 5^{th} *ed.*. A. Jeffrey, Ed. San Diego CA: Academic, 1994.

[14] A.G. Zajić and G.L. Stüber, "3-D MIMO mobile-to-mobile channel simulation," *16th IST Mobile & Wireless Communications Summit*, Budapest, Hungary, July 2007.

[15] K. V. Mardia and E. P. Jupp, *Directional Statistics*. New York. Wiley 1999.

[16] G. Acosta, K. Tokuda, and M. A. Ingram, "Measured joint Doppler-delay power profiles for vehicle-to-vehicle communications at 2.4 GHz," *Proc. IEEE GLOBECOM'04*, vol. 6, pp. 3813–3817, Dallas, TX, Nov. 2004.